Proceedings of ERAD 2006

A variational method to reduce the sidelobe contamination of bistatic Doppler measurements

Nabil Lamrani, Michel Chong

Laboratoire d'Aérologie, UMR 5560 (CNRS/UPS), Toulouse (France).

Abstract. This study proposes a solution to correct for contamination of bistatic measurements of a dual-Doppler monostatic-bistatic radar network. A variational method is developed in order to reconstruct bistatic Doppler velocities, even though the actual wind vector is unknown, using both the monostatic and bistatic observations.

The evaluation of the method is performed as follows: 1) generation of radar measurements based on a numerical simulation of a West African squall line through the non-hydrostatic Meso-NH model; 2) application of the bistatic measurements' correction; and 3) retrieval of the 3D wind field using the multiple-Doppler synthesis and continuity adjustment technique (MUSCAT). Accuracy of the retrieved horizontal wind field is evaluated by comparing with the Meso-NH simulation taken as a reference.

It is shown that the errors are 40 % less important on average than in a simulated dual-Doppler network not using the bistatic measurements' correction.

1 Introduction

Since the work of Wurman et al (1993), it has been shown (de Elía and Zawadzki, 2001; Friedrich and Hagen, 2004) that bistatic Doppler receivers present advantages to several Doppler radar system and particularly to monostatic multiple-Doppler radar system as simultaneous measurements of Doppler velocities can be realized and high costs of such equipments can be reduced. A bistatic multiple-Doppler network consists of one traditional transmitting Doppler radar and one (or more) passive, low gain, nontransmitting, nonscanning radar receivers at remote sites. Then with two or more bistatic Doppler measurements within storms, this network combined with an adaptated data processing chain including a variational method, can provide a full wind field determination over a particular area.

But bistatic Doppler network's approach presents disadvantages as shown by de Elía and Zawadzki (1999). The use of low-gain receiving antenna can cause the receiving sites to be less sensitive than the traditional high-gain radars at comparable range. Moreover, the wide viewing angles of this receiver's antenna make it more sensitive to multiple scattering contamination and to sidelobe contamination (SICO). The monostatic transmitter/receiver gives information on radar reflectivity and Doppler velocities for a weather volume using the backscattered information. The energy of the return radar signal is proportional to the square of the gain radar beam; sidelobes do not influence the monostatic measurements in a first approximation. In the case of bistatic measurements, the contribution of scattered signal from sidelobes can be non negligible and thus it can yield observations of bistatic reflectivity and Doppler velocity to be greatly biased.

The degree of contamination in the data measured by the bistatic receivers depends strongly on weather conditions. Elía and Zawadzki (2000) showed that it is linked to strong reflectivity gradient areas like bright band in stratiform case or a core of convective storm. In these conditions, 3D wind field reconstruction performed with Doppler data from bistatic network may lead to false wind components in specific areas.

Elía and Zawadzki (2000) proposed to use a model to correct for the contamination of bistatic reflectivity. In this study, we present a method to reduce the contribution of sidelobes effects to the measurements of bistatic Doppler velocity.

Correspondence to: Nabil Lamrani.

lamn@aero.obs-mip.fr

2 Expression of bistatic measurements

All this part is based on the formalisms described by Elía and Zawadzki (2000) and Doviak and Zrnic (1993).

The bistatic receiver get all the signal that enter the aperture of its antenna at a time t, *i.e.* that travelled a distance $r = ct$ where c is the light celerity, *i.e.* all contribution located on an ellipsoid of constant time delay defined by $r_1 + r_2 = r = cste$, where r_1 refers to the transmitter-target distance and r_2 to the target-receiver distance.

Bistatic antenna measures a reflectivity which is given by:

$$\overline{Z}_{mm\ ^6m^{-3}} = \frac{\int_V Z\,(r_1', \Phi', \theta').\ I\,(r_1', \Phi', \theta')\,dV}{\int_V I\,(r_1', \Phi', \theta')\,dV} \quad (1)$$

and an apparent Doppler velocity $\overline{V}_a$ defined by:

$$\overline{V}_a(r_1,\Phi,\theta) = \frac{\int_V V_a(r_1',\Phi',\theta').Z(r_1',\Phi',\theta').I(r_1',\Phi',\theta').dV}{\int_V Z(r_1',\Phi',\theta').I(r_1',\Phi',\theta').dV} \quad (2)$$

with:

$$I = \frac{G_m(\Phi'-\Phi, \theta'-\theta).G_b(\beta', \theta_b')\cos^2\gamma}{r_1^2 r_2^2}$$

where Z is the radar reflectivity, I is the gain factor of the receiver, dV the resolution volume, G_m and G_b respectively monostatic and bistatic antenna gain. r_1, Φ and θ refer to the pointing parameters of the monostatic antenna, when r_2, β and θ_b refer to bistatic antenna ones. Primed symbols in (1) and (2) refer to all target's contribution present within dV. γ is the monostatic-target-bistatic angle.

(1) and (2) are weighted average values of impact point of the signal emitted by the monostatic on a given ellipsoid of constant time delay. Let $\omega(r_1,\Phi,\theta)$ be the generated individual weights contributing to $\overline{V}_a$. So (1) becomes:

$$\overline{V}_a(r_1,\Phi,\theta) = \int_V V_a(r_1',\Phi',\theta').\omega(r_1',\Phi',\theta')dV \quad (3)$$

with:

$$\omega(r_1,\Phi,\theta) = \frac{Z(r_1,\Phi,\theta).I(r_1,\Phi,\theta)}{\int_V Z(r_1',\Phi',\theta').I(r_1',\Phi',\theta')dV'}$$

3 Reconstructing bistatic Doppler velocities

With a regular sampling from the monostatic radar (*i.e.* both in elevation and azimuth) forming a succession of constant elevation cones, each cone containing a defined number of radials, bistatic sampling can be seen as a distribution of points on a given ellipsoid of constant time delay function of the pointing angles and the distance to the ellipsoid. Let be $\overline{V}_a(r_{1i},\Phi_j,\theta_k)$ this distribution. Index *i* refers to the number of bistatic measurement points on a monostatic radial (at a distance r_1), *i. e.* the number of the ellipsoid, *j* refers to the azimuth relative to the monostatic radials that are in the bistatic aperture and *k* refers to the elevations. Then for a given *i* ellipsoid we have:

$$\overline{V}_a(j,k) = \sum_{k'}\sum_{j'} V_a(j',k').\omega(j',k') \quad (4)$$

with:

$$\omega(j',k') = \frac{Z(j',k').I(j',k')}{\sum_{k'}\sum_{j'} Z.I}$$

Those weights are calculated using monostatic measurements interpolated at bistatic measurements points.

(4) expresses the measured $\overline{V}_a$ as function of unknown "actual" velocity V_a. It forms an underestimated system which can be solved by using a variational analysis (least square with regularization constraint) if we minimize the following functional F for each ellipsoid:

$$F = \left[\sum_{k'}\sum_{j'} V_a(j',k').\omega(j',k') - \overline{V}_{ai}\right]^2 + \mu.C \quad (5)$$

The regularisation constraint C can have the following form:

$$C = \int\left\{\left(\frac{\partial^2 V_a}{\partial\Phi^2}\right)^2 + \left(\frac{\partial^2 V_a}{\partial\theta^2}\right)^2 + 2\left(\frac{\partial^2 V_a}{\partial\Phi\,\partial\theta}\right)^2\right\}d\Phi\,d\theta$$

which acts as a low pass filter.

4 Results

4.1 Sidelobes effects

In order to test this variational method, simulated monostatic and bistatic radar measurements have been generated using a meso-NH simulation of an African squall line (Fig. 1.). It presents a squall line of 400 km extension in a north-west south-east direction where the radars can be positioned and then virtually sample the system. Radars are positioned in a north-south axis located 30 km apart. The bistatic is oriented 60° in azimuth and the monostatic samples are obtained every 1° in azimuth and in different elevation sites within the convective zone.

Two datasets are considered. The first uses the complete radar beam patterns (including sidelobes) and it is refered to as "real" dataset. The second one does not use the complete monostatic beam pattern but an ideal (not real) diagram only including the central peak without main lobe extension or sidelobes, and it is called "ideal" dataset.

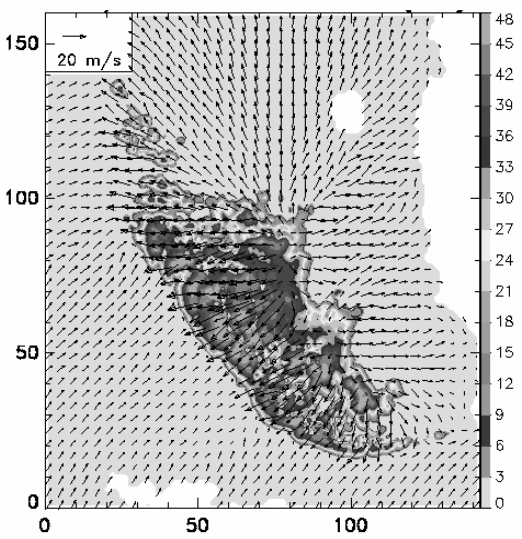

Fig. 1. The meso-NH simulation of an African squall line used to generate simulated data. Reflectivity is given by the right greyscale and the wind is given by the vector field on a grid mesh.

The method presented in section 3 is applied to "real" bistatic measurements in order to obtain the "corrected" dataset. Then "ideal", "real" and "corrected" data are used to retrieve the 3D wind components with MUSCAT (Bousquet and Chong, 1998). Fig. 2. shows the wind fields in the "ideal" and "real" case, at 7 km altitude.

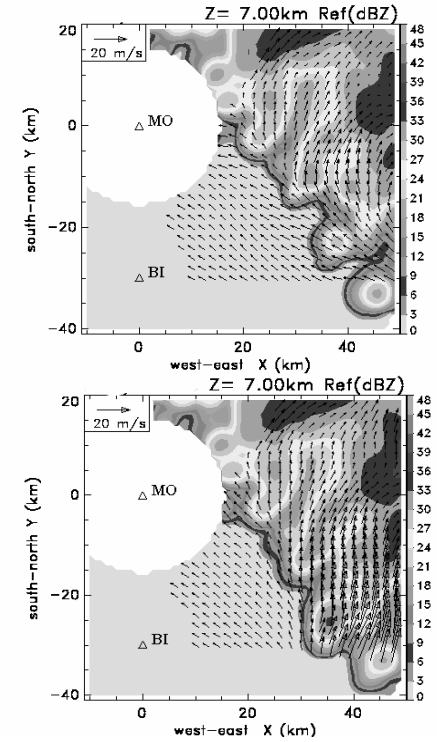

Fig. 2. In the upper panel, the MUSCAT retrieval of 3D wind and reflectivity field with an "ideal" dataset. In the lower panel, the retrieval using the "real" simulated dataset.

Fig. 2. presents how sidelobes contamination influences the retrieval by over estimating bistatic "real" measurements and then leads to a false retrieval of the wind vector field in some areas.

4.2 Corrected vs uncorrected fields

A first approach to estimate our correction method is to calculate the difference between the reference wind fields (meso-NH simulation) and the ones retrieved with the "ideal", "real" and "corrected" datasets. Fig. 3. presents those differences on the u component at 7 km altitude.

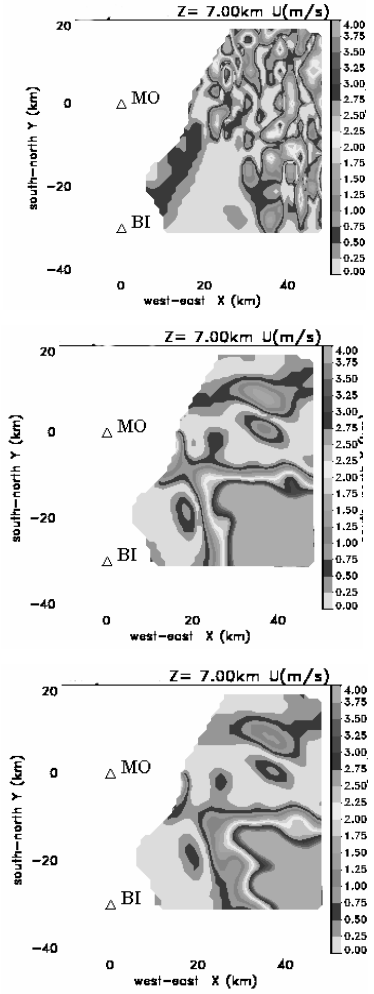

Fig. 3. Errors on the estimation of the *u* wind component in the "ideal" case (upper panel), the "real" case (middle panel), the "real and corrected" case (lower panel) at 7 km altitude.

In the "ideal" case, we can see the errors due to the retrieval done by MUSCAT and how important these are in first planes. This result is well documented in Bousquet and Chong (1998). The next cases show how the correction influences the retrieval. SICO subsist but qualitatively reduced by the correction of bistatic measurements.

To quantify this amelioration a first way is to set comparisons between "corrected" and "ideal" retrieved *u* component and between not "corrected" and "ideal" retrieved *u* component. This work is presented in Fig. 4.

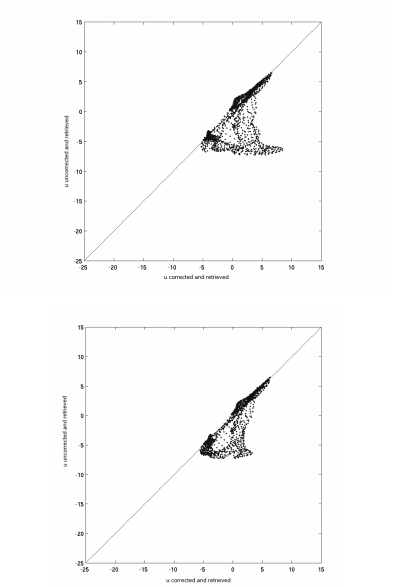

Fig. 4. In the upper panel, the comparison between the not "corrected and retrieved" *u* components and the "ideal" ones. In the lower one, the same comparison with the "corrected and retrieved" case.

It appears that the method filters a part of the not well retrieved values of *u* but SICO is still present. Notice that the same study has been realized with the *v* component and that a stratiform case in the simulation have been also realized to verify those effects. The same results have been found.

A final analysis has been done in order to estimate the method contribution. This result is presented in Fig. 5.

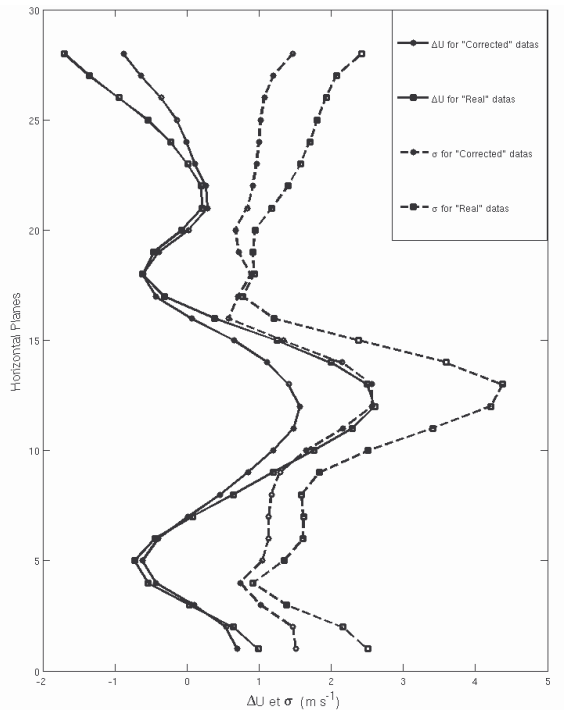

Fig. 5. Statistic evaluation of the method. Solid lines refer to the average error per horizontal retrieved plane Δ*u* in the uncorrected case (square marker) and in the corrected case (spot markers). The corresponding standard variations σ are in dashed lines

It shows the average of the error Δ*u* on each horizontal plane and its standard variation with (solid line) and without correction (dashed line). We can see how the standard variation is maximum and how not "corrected" component is over estimated in the planes corresponding to the bright band witch present a strong gradient of reflectivity (Elía and Zawadzki, 2000). It also shows how the correction reduces SICO in those areas. It leads us to conclude on an improvement of about 40% in the estimation of the horizontal wind field and that errors can be reduced to less than 2 $m.s^{-1}$.

5 Conclusion

SICO phenomena induces false retrieval of 3D wind vector with the dual-Doppler technique. The variational method permits to reduce this effect. Contaminated bistatic measurements can be corrected at a range of 40% even though the retrieved wind vector is not known. Then a complete data processing chain of a bistatic network should include this improvement in order to reduce SICO before applying constraining data models based on the index of contamination or the reflectivity gradient.

References

Bousquet, O., and M. Chong, 1998: A Multiple-Doppler and Continuity Adjustment technique (MUSCAT) to recover wind components from Doppler radar measurements. *J. Atmos. Oceanic Technol.*, **15**, 343-359

de Elía, R., and I. Zawadzki, 2000: Sidelobe contamination in bistatic radars. *J. Atmos. Oceanic Technol.*, **17**, 1313-1329

de Elía, and Zawadzki, 2001: Optimal layout of a bistatic radar network. *J. Atmos. Oceanic Technol.*, **18**, 1184-1194

Friedrich, K., and M. Hagen, 2004: Evaluation of wind measured by a bistatic Doppler radar network. *J. Atmos. Oceanic Technol.*, **21**, 1840-1854

Protat, A., and I. Zawadzki, 1999: A variational method for real-time retrieval of three-dimensional wind field from multiple-Doppler bistatic radar network data. *J. Atmos. Oceanic Technol.*, **16**, 432-449

Satoh, S., and J. Wurman, 2003: Accuracy of wind field observed by a bistatic Doppler radar network. *J. Atmos. Oceanic Technol.*, **20**, 1077-1091

Wurman, J., 1994: Vector winds from a single-transmitter bistatic dual-Doppler radar network. *Bull. Amer. Meteor. Soc.*, **75**, 983-994.

Wurman, J., S. Heckman, and D. Boccippio, 1993: A bistatic multiple Doppler network. *J. Appl. Meteor.*, **32**, 1802-1814